NASA Technical Memorandum 104326

Flight and Static Exhaust Flow Properties of an F110-GE-129 Engine in an F-16XL Airplane During Acoustic Tests

Jon K. Holzman, Lannie D. Webb, and Frank W. Burcham, Jr.
NASA Dryden Flight Research Center
Edwards, California

1996

National Aeronautics and
Space Administration

Dryden Flight Research Center
Edwards, California 93523-0273

CONTENTS

TABLES

FIGURES

ABSTRACT

The exhaust flow properties (mass flow, pressure, temperature, velocity, and Mach number) of the F110-GE-129 engine in an F-16XL airplane were determined from a series of flight tests flown at NASA Dryden Flight Research Center, Edwards, California. These tests were performed in conjunction with NASA Langley Research Center, Hampton, Virginia (LaRC) as part of a study to investigate the acoustic characteristics of jet engines operating at high nozzle pressure conditions. The range of interest for both objectives was from Mach 0.3 to Mach 0.9. NASA Dryden flew the airplane and acquired and analyzed the engine data to determine the exhaust characteristics. NASA Langley collected the flyover acoustic measurements and correlated these results with their current predictive codes. This paper describes the airplane, tests, and methods used to determine the exhaust flow properties and presents the exhaust flow properties. No acoustics results are presented.

NOMENCLATURE

A8	exhaust nozzle physical area at the throat, in^2
A9	exhaust nozzle physical area at the exit plane, in^2
AE8	exhaust nozzle effective throat area, in^2
AE9	exhaust nozzle effective exit-plane area, in^2
AFFTC	Air Force Flight Test Center, Edwards AFB, California
AGL	above ground level
ANOPP	Aircraft Noise Prediction Program
CTC	climb to cruise
EGT	exhaust gas temperature downstream of the turbine, °R
Fg	gross thrust, lbf
GAM7	specific heat ratio of exhaust gas at nozzle entrance
jet	location where exhaust flow has expanded to ambient pressure
M9	nozzle exit Mach number based on nozzle expansion ratio
Mjet	fully expanded *jet* Mach number
Mach	Mach number
Meas	measured
NPR	nozzle pressure ratio (*P8/Pamb*)
N1	fan rotor speed, rpm
N2	core rotor speed, rpm
OH	overhead
P1	engine face total pressure, lbf/in^2
Ps3	compressor discharge static pressure, lbf/in^2
PT2.5	fan discharge total pressure, lbf/in^2

P7	exhaust nozzle entrance total pressure, lbf/in^2
P8	exhaust nozzle throat total pressure, lbf/in^2
Pamb	ambient static pressure, lbf/in^2
PLA	power lever angle, deg
PLF	power for level flight
Ps9	exit plane static pressure, lbf/in^2
Tamb	ambient temperature, deg
T1	engine face total temperature, °R
T8	exhaust-nozzle mixed *jet* total temperature at the throat, °R
Ts9	exhaust nozzle exit static temperature, °R
Tsjet	fully expanded *jet* static temperature, °R
V9	velocity at nozzle exit, from *M9*, ft/sec
Vjet	fully expanded nozzle *jet* velocity, ft/sec
WFE	core engine fuel flow, lb/h
W8	mass flow rate at the exhaust nozzle throat, lb/sec

INTRODUCTION

Exhaust flow properties (mass flow, temperature, pressure, velocity, and Mach number) of an engine are key in determining the acoustic characteristics. Airport noise is one of the key issues in determining the environmental acceptability of proposed supersonic transport airplanes. These airplanes will probably be powered by engines operating at high nozzle pressure ratios (NPR) and high exhaust *jet* velocities. Concern exists not only for noise produced during takeoff and landing but also for noise produced along the flightpath of the airplane during the subsonic portion of the climb out for a distance of up to 50 miles.

To determine the engine noise for these transport designs, acoustic codes, such as the Aircraft Noise Prediction Program (ANOPP), are used.[1] These codes were developed and validated using data acquired from engines with NPR's and flight speeds lower than that planned for supersonic transports. Doppler amplification of the shock noise in the forward approach arc of the vehicle flightpath was of particular concern.

For these reasons, NASA Langley Research Center, Hampton, Virginia (LaRC), and Dryden Flight Research Center, Edwards, California, jointly conducted tests to acquire in-flight acoustic data for high NPR engines. Results of these tests would be used to update and validate the current noise predictive codes. The two main flight test objectives were to assess subsonic climb-to-cruise (CTC) noise using an aircraft with high NPR engines and to obtain an improved noise database to validate the ANOPP and other noise predictive codes. The test airplanes included an F-18 powered by two F404-GE-400 engines, (General Electric Company, Lynn, Massachusetts) and an F-16XL, ship 2, powered by a single F110-GE-129 engine (General Electric Company, Evendale, Ohio). The F-18 exhaust characteristics were presented in reference 2. NASA Dryden responsibilities for the F-18 airplane are discussed in reference 3. For the F-16XL, ship 2 tests, the responsibilities were to plan and conduct the flyover tests, record and analyze the flight data, determine the airplane space position, determine the engine exhaust gas flow properties, and conduct a ground static acoustic survey. NASA Langley responsibilities were to setup the microphone array, record the noise measurements, merge the acoustic and space position data, analyze and evaluate the acoustic data, and correlate these data with Dryden-determined engine exhaust properties. The preliminary acoustic results are presented in the footnoted report.*

The F-16XL, ship 2, study consisted of flights over a microphone array at varying speeds and altitudes. Two types of flight tests were conducted: subsonic CTC noise determination and ANOPP predictive code validation. In the subsonic CTC portion of the study, flyovers were conducted at altitudes from 3,800 to 12,300 ft and from Mach 0.3 to Mach 0.95 all at an intermediate (maximum nonafterburning) power setting. For the ANOPP evaluation flyovers, the tests were flown at 3,800 ft and from Mach 0.3 to Mach 0.95. A static ground-level engine-run test was also conducted over the power setting range from idle to intermediate power in order to establish baseline exhaust acoustic noise levels with no forward airplane velocity.

This paper describes the F-16XL airplane and F110-GE-129 engine, presents the flight tests performed using the F-16XL airplane, documents the test and analysis techniques used to calculate the engine flow properties, and presents the engine exhaust flow properties. Acoustics data are not presented. Use of trade names or names of manufacturers in this document does not constitute an official endorsement of such products or manufacturers, either expressed or implied, by the National Aeronautics and Space Administration.

F-16XL AIRCRAFT DESCRIPTION

The F-16XL airplane has a "cranked" delta wing and is an extensive modification of the F-16 airplane (fig. 1). Two aircraft were built by Lockheed-Martin (formerly General Dynamics, Fort Worth, Texas). The F-16XL, ship 2, a two-seat aircraft, has a length of 54.2 ft, a wingspan of 34.3 ft, and a maximum weight of approximately 36,000 lb. Figure 1(a) shows an in-flight photograph and figure 1(b) shows a three-view drawing with key dimensions of this airplane. It has a maximum Mach number of approximately 2.05 and a nominal design load factor of 9 *g* which provides a large performance envelope for flight research. The F-16XL, ship 2, aircraft is powered by a single F110-GE-129 afterburning turbofan engine mounted in the rear fuselage.

Inlet Description

The F-16XL, ship 2, air inlet consists of a normal shock inlet mounted below the front fuselage followed by an S duct to the engine. Inlet size and pressure recovery characteristics are important in determining the engine exhaust flow conditions. A front view of the inlet is shown in figure 2(a). The inlet has a geometric capture area of 893 in^2. This area is 56 in^2 larger than the F-16 A/B small inlet but slightly smaller than the F-16 C/D big inlet. Figure 2(b) shows the total pressure recovery of this inlet, as determined from wind-tunnel tests, for a range of engine-corrected airflows and Mach numbers.

*Jeffrey J. Kelly, Mark R. Wilson, John Rawls Jr., Thomas D. Norum, and Robert A. Golub, *F-16XL and F-18 High Speed Acoustic Flight Test Data Base*, NASA CD TM-10006, 1996. (This is a controlled distribution document. Direct inquiries to the author of this document at NASA Langley Research Center Aeroacoustics Division.)

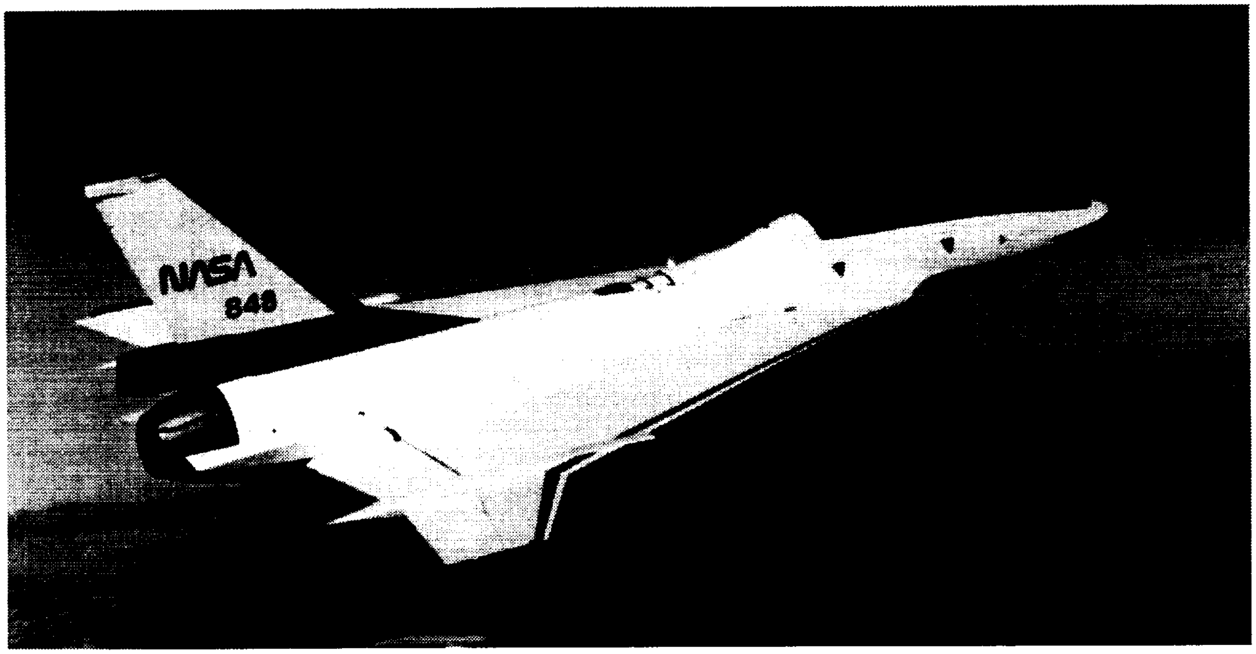

EC-91-646-1

(a) In-flight photograph.

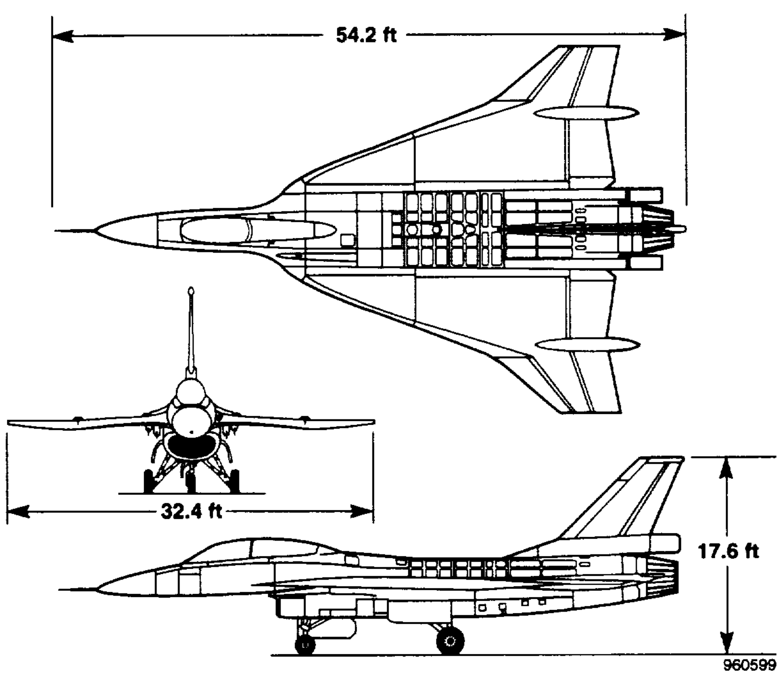

(b) Three-view drawing.

Figure 1. The F-16XL, ship 2, airplane.

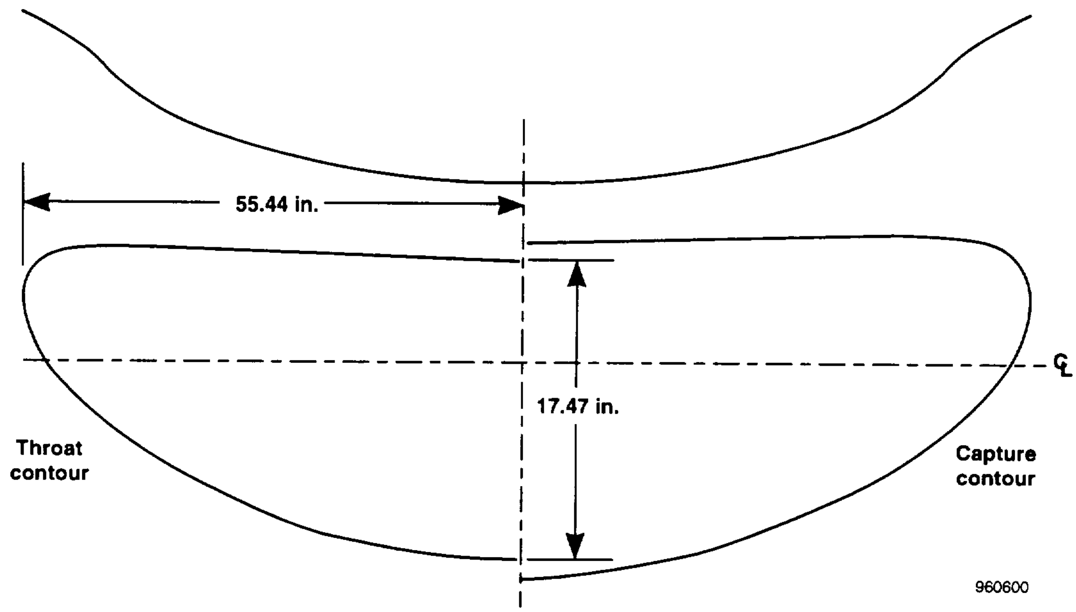

(a) Drawing of the inlet capture area and throat area.

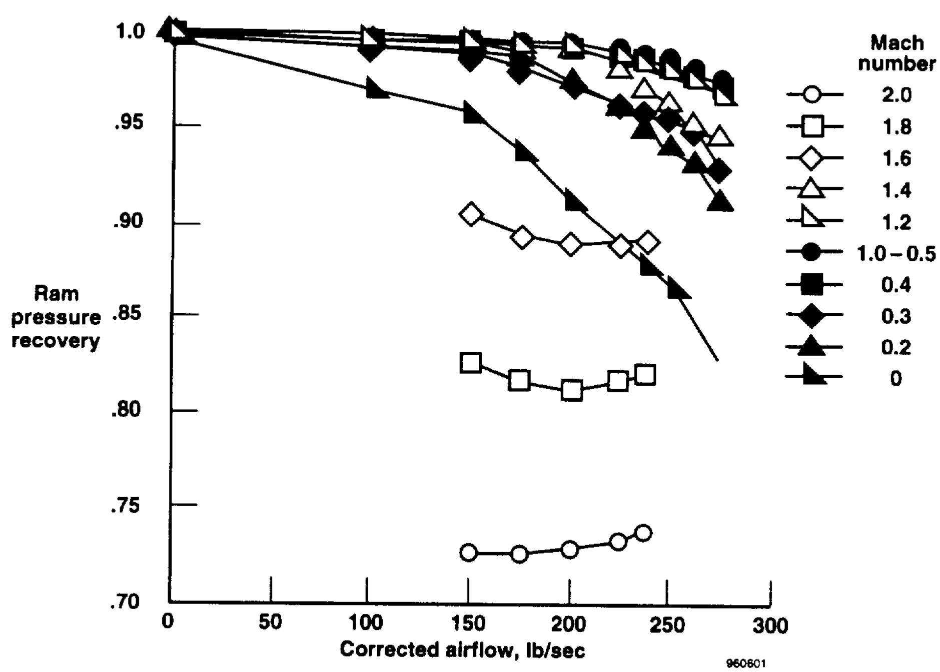

(b) Inlet ram pressure recovery.

Figure 2. The F-16XL, ship 2, inlet (893 in^2 capture area).

Engine Description

For the acoustic tests, the F-16XL, ship 2, was powered by the F110-GE-129 increased performance engine. This two-spool, low-bypass, axial-flow turbofan engine with afterburner has a maximum thrust of 29,000 lbf. Figure 3 shows a cut away schematic view of the engine depicting the station designations, including the "*jet*" station where the engine exhaust flow has adjusted to free stream static pressure. The engine features a three-stage fan driven by a two-stage, low-pressure turbine and a seven-stage, high-pressure compressor driven by a single-stage, high-pressure turbine. Variable inlet guide vane geometry is incorporated into the fan and the first four stages of the high-pressure compressor. A fan/core mixer is just upstream of the afterburner. The exhaust nozzle is of the convergent-divergent type with a variable throat area. The engine is equipped with a digital engine control unit which controls the fuel flows, rotor speeds, variable geometry, pressures, and temperatures in the engine. Idle power is at 20° power lever angle (PLA) setting, and intermediate (maximum nonafterburning) power is at 85° PLA. At this latter setting, the engine produces NPR similar to those proposed for some versions of future supersonic transport engine designs.

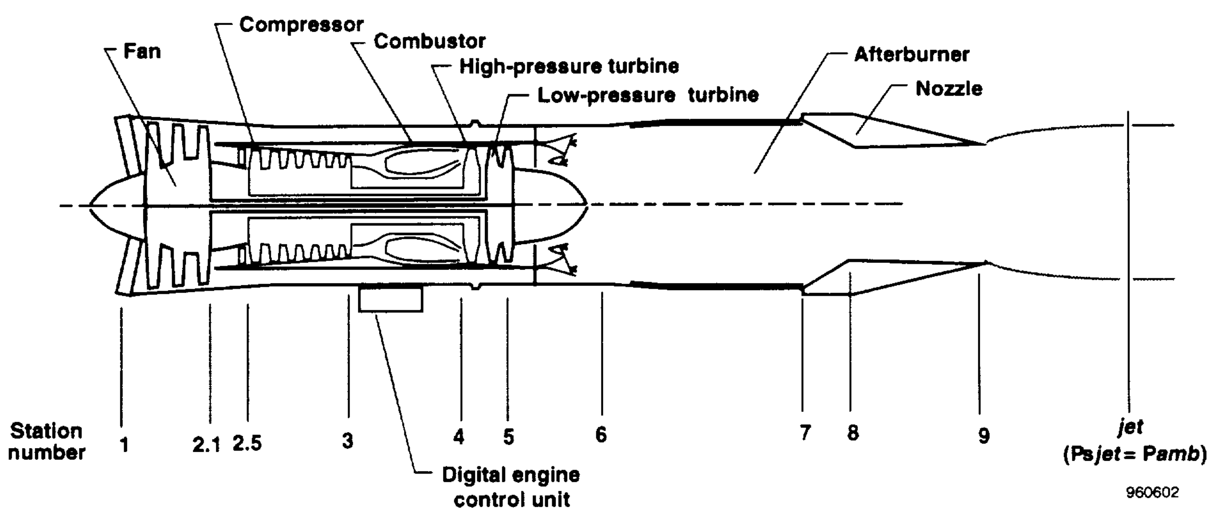

Figure 3. Cutaway view of the F110-GE-129 engine and station designations.

MEASUREMENTS

The F-16XL, ship 2, airplane was instrumented to measure parameters of interest for the acoustic flyover test. Aircraft and engine parameters were included. In addition, acoustic, meteorological, and airplane space-positioning measurements were made on the ground.

Aircraft

The F-16XL, ship 2, Mach number and altitude were obtained from the pitot-static probe on the noseboom. Pressures from the pitot probe were fed to the central airdata computer where Mach number and altitude were calculated. The aircraft also had an inertial navigation system for accurate velocity and position determination which was helpful in flying the airplane as close as possible to the designated ground-track profile over the Edwards, California, fly-by line. Angle of attack and angle of sideslip were measured by vanes on the noseboom. These data were recorded at 10 samples/sec onboard on a 10-bit pulse code modulation (PCM) data system and were also transmitted to the ground. The airplane was equipped with a C-band radar beacon to aid in precise space positioning.

Engine

The F110-GE-129 engine was extensively instrumented. For this paper, the parameters of interest are those used as inputs to and for comparison with the F110-GE-129 engine deck and for the acoustic analysis. These parameters include PLA; engine face total temperature, *T1*; fan discharge total pressure, *PT2.5*; compressor discharge static pressure, *Ps3*; core engine fuel flow, *WFE*; fan rotor speed, *N1*; core rotor speed, *N2*; engine exhaust gas temperature (EGT); and exhaust nozzle physical area at the throat, *A8*.

Acoustics Measurements

Flyover Tests

For the CTC and ANOPP tests, the acoustic data were measured with an analog and digital microphone array positioned along the flyby line on Rogers Dry Lakebed (fig. 4). This location provided a good proximity to the tracking radar, an adequate distance from the Edwards, California, main runway, and a large flat area suitable for acoustics measurements. The analog microphone setup was similar to the setup used by NASA Dryden during the static ground-run engine acoustic test.

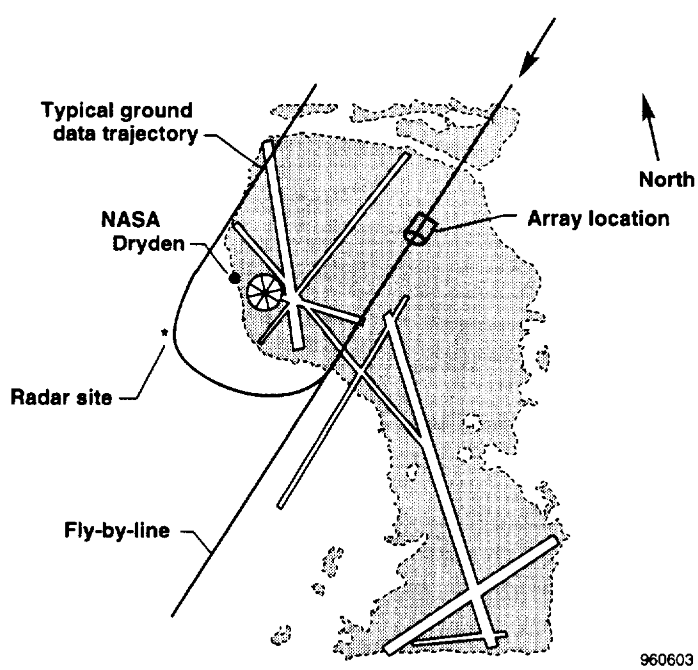

Figure 4. Ground track and array layout on Rogers Dry Lake, Edwards, CA.

Flyover Space Positioning

The NASA Dryden FPS-16 radar was used to track the radar beacon on F-16XL, ship 2, airplane during the acoustic flyovers. These data were used in the control room to assist the pilot in lineup, establish the time for beginning and completing data runs, and determine the validity of the track for each flyover. These data were also used by NASA Langley in the postflight analysis to determine the position of the airplane for correlation with the microphone data.

Static Acoustic Tests

For the static tests conducted by NASA Dryden, a 24-microphone array was located on a large flat taxiway area (fig. 5). Nominal microphone placement was every 7.5° on an arc 99 ft from the engine exhaust centerline. Inverted microphones were mounted inside windscreens with the diaphragms 0.5 in. above a thin aluminum plate which was taped to the concrete or asphalt surface. This setup allowed for measuring acoustic exhaust noise free of ground reflections.

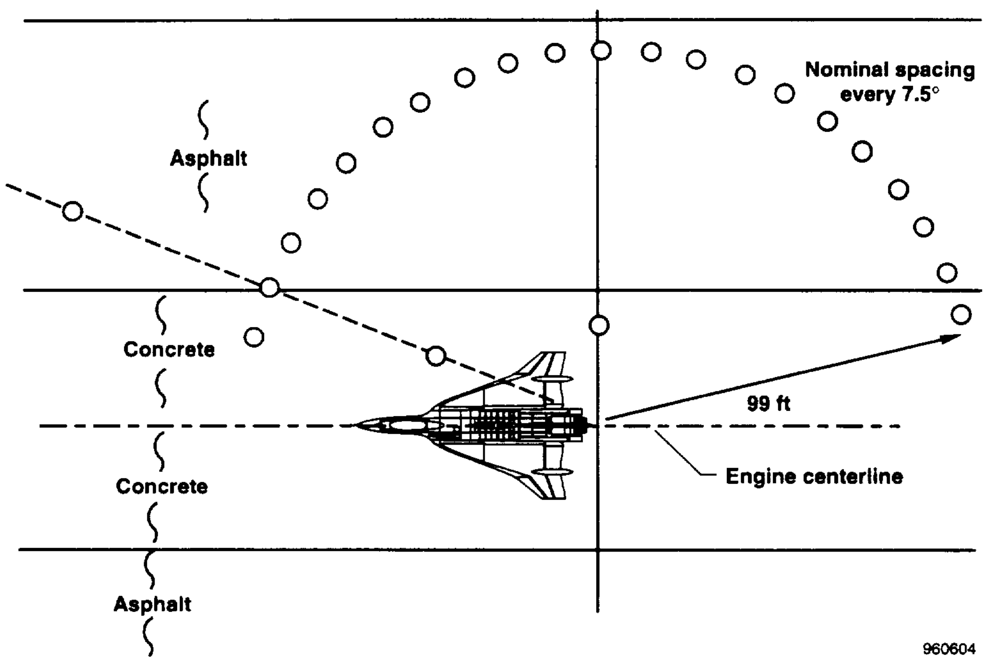

Figure 5. Microphone array for the F-16XL, ship 2, ground static acoustic survey.

Figure 6 shows the airplane positioned for the static test. Three of the microphones are visible. The NASA Dryden acoustics van was used to record the 24 channels of microphone data. Two 14-track tape recorders were installed in the mobile trailer. Twelve channels of acoustic data were recorded on each of the two recorders; meanwhile, the remaining two channels were used to record the time and the pilot's event marker. Each of the 24 microphone stations was battery powered and consisted of a condenser microphone, a preamplifier, and a line driver amplifier. Each station was connected to a separate line driver by 1000 ft of shielded, coaxial signal cable. The line driver signal was in turn connected to one of the recorder data channels in the trailer, using a 1000-ft length of neoprene-covered cable containing a shielded, twisted pair of copper signal wires. The trailer also contained a weather station for recording local temperatures as well as wind velocity and direction in the area of the microphone array and radios for communication with the airplane.

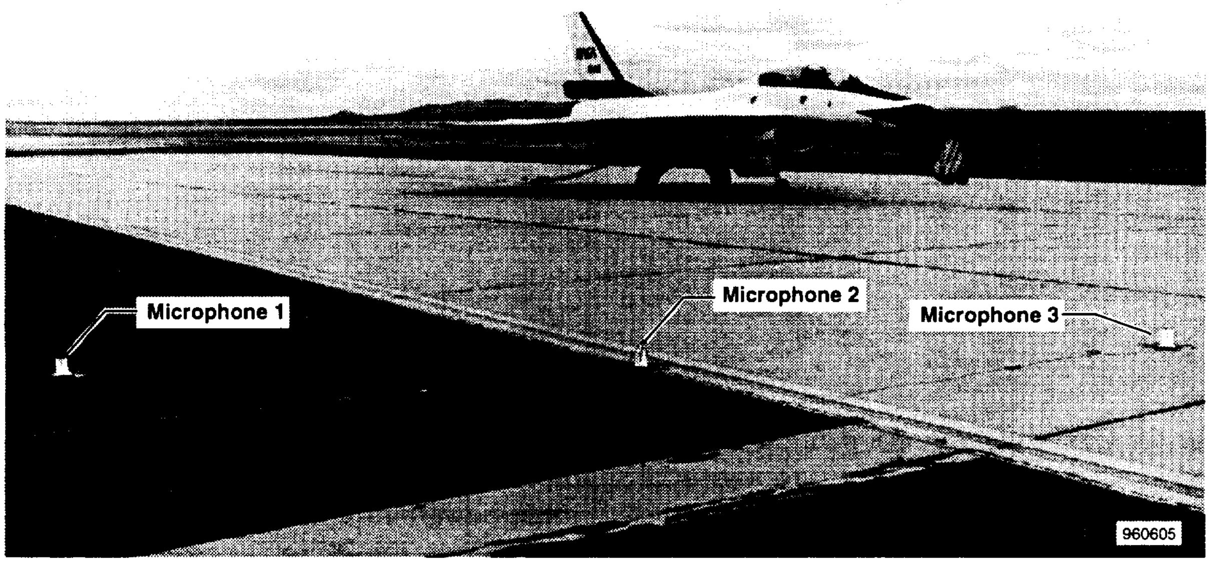

Figure 6. Photograph of the F-16XL, ship 2, ground acoustic test showing 3 microphones in foreground.

Meteorology

Atmospheric properties affect the propagation of acoustics and are one of the inputs into the ANOPP. Conditions for the flight data were determined from four sources:

1. The F-16XL, ship 2, onboard measurements
2. The weather balloons
3. A ground weather station at the acoustics van
4. A tethered balloon located near the flyover array

The onboard measurements were primarily winds aloft data readout from the airplane inertial system and $T1$. The tethered balloon was raised and lowered periodically during the tests using a 1500-ft tether.

TEST PROCEDURES

To satisfy dual objectives of the program, two flight tests were conducted: subsonic CTC noise determination and ANOPP predictive code validation. In both cases, obtaining acoustic data during the period when the airplane was more than 10° to 15° above the horizon as measured from the center of the acoustic array was desired. Distances of the start and end points away from the acoustic array were, therefore, a function of the test altitude. At the lowest test altitude, 1500 ft above ground level (AGL), this distance was approximately 1 mile. The pilot flew along the fly-by line using a combination of visual navigation, onboard inertial navigation, and callouts from the control room.

Climb-To-Cruise Tests

The flight matrix for the CTC runs consisted of level flight accelerations over the acoustic array at various Mach numbers and altitudes. During these runs, the engine power setting was constant at 85° (intermediate) in order to obtain the maximum engine NPR. Table 1 lists the CTC desired test conditions. Test altitudes desired varied from an altitude of 3,800–32,300 ft, and the Mach numbers ranged from 0.30 to 0.90.

Table 1. Climb-to-cruise test points.

Mach number	Altitude, ft
0.3	3,800
0.6	7,300
0.65	12,300
0.75	22,300
0.9	32,300

For the CTC condition, the pilot first stabilized the aircraft at the desired altitude and just below the desired Mach number. As the airplane approached the acoustic start point, based on a radio call from the control room, the throttle was advanced to the intermediate power setting. Then the engine was allowed to stabilize for approximately 5 sec before the start of the test run. The aircraft would accelerate depending on the degree of excess thrust through the desired test conditions in level flight. Some acoustic runs were initiated directly over the center of the array with the run terminating when the elevation angle was again 15° above the horizon. At some flight test conditions, the aircraft speed brakes were deployed to reduce the acceleration during the acoustic data acquisition. Because of aircraft acceleration no data were obtained at the 22,300 and 32,300 ft altitudes for the F-16XL, ship 2, tests.

ANOPP Tests

The ANOPP code evaluation tests were flown at constant Mach number and at an altitude of 3800 ft (1500 ft above the local ground level). Test Mach numbers ranged from 0.30 to 0.95 (table 2). For the ANOPP tests, the throttle setting was the power level flight (PLF) at constant speed and varied from about 35° to 57°. For these runs, the pilot was vectored over the microphone array in similar fashion to the CTC tests. Once power was set, it was not changed during the flyover, so small changes in Mach number occurred. Speed brakes were not used for ANOPP tests.

Table 2. ANOPP test points.

Mach number	Altitude, ft	Power setting, deg
0.3	3800	~ 48°
0.6	3800	~ 35°
0.8	3800	~ 47°
0.95	3800	~ 56°

Table 3 shows the CTC and ANOPP tests that were flown during three flights. Note that all of the CTC tests resulted in a significant change in Mach number during the run, which was caused by the excess thrust. Repeat tests were flown at some conditions. The data shown with table run letters were the primary acoustics tests for CTC and ANOPP tests. Exhaust flow properties from these tests are shown in table 4.

Table 3. Acoustics flight tests for the F-16XL, ship 2.

Test for table in this report	Mach number start–end	Altitude, ft	Run legs, mi	Run type
		Flight 1		
A	0.33–0.75	~3,800	±2	CTC
B	0.58–0.95	~7,300	±4	CTC
C	0.70–0.92	~12,300	±7	CTC
D	0.31–0.79	~3,800	±2	CTC
		Flight 2		
	0.31–0.61	~3,800	±2	CTC
	0.34–0.55	~3,800	±2	CTC
	0.31–0.48	~3,800	0 to –2	CTC
	0.32–0.47	~3,800	0 to –2	CTC
	0.60–0.73	~7,300	±4	CTC
		Flight 3		
	0.33–0.33	~3,800	±2	ANOPP
E	0.31–0.28	~3,800	±2	ANOPP
	0.61–0.58	~3,800	±2	ANOPP
F	0.60–0.60	~3,800	±2	ANOPP
G	0.80–0.81	~3,800	±2	ANOPP
	0.80–0.80	~3,800	±2	ANOPP
H	0.95–0.95	~3,800	±2	ANOPP
	0.94–0.95	~3,800	±2	ANOPP
	0.30–0.58	~3,800	±2	CTC
	0.28–0.59	~3,800	±2	CTC
	0.28–0.49	~3,800	±2	CTC
	0.31–0.50	~3,800	0 to 2	CTC

Static Tests

For the static tests, the F-16XL, ship 2, aircraft was tied down, and engine power setting was varied to achieve engine pressure ratio increments of 0.1 from idle to intermediate power (98.5 percent $N2$) and then back to idle. At each test point, the engine was allowed to stabilize for 1 min; then acoustic data were acquired for 30 sec. These tests were conducted with the wind speed below 5 kn to minimize wind noise. Atmospheric data were obtained from the NASA Dryden acoustics van and from the Air Force Flight Test Center (AFFTC), Edwards, California, observations.

ANALYTICAL TECHNIQUES

Engine Exhaust Flow Properties

Jet-mixing and shock cell noise are two primary sources of noise for high-NPR engines during take-off and subsonic climb (ref. 2). These noise sources are primarily affected by the aircraft velocity, exhaust-exit Mach number and velocity, and NPR. For acoustic analysis, exhaust characteristics are often defined at the nozzle exit (station 9) and also at an assumed fully expanded condition (station *jet*) (fig. 3). Jet-mixing noise is primarily a function of the difference between the fully expanded nozzle jet velocity, *Vjet*, and the free stream velocity. Shock cell noise is a function of the difference between the fully expanded jet Mach number, *Mjet*, and the nozzle exit Mach number based on nozzle expansion ratio, *M9*. At the point where *M9* = *Mjet*, the shock cell noise is diminished. Nozzle exit velocity from nozzle exit, *V9*, and Mach number *M9* are based on the aerothermodynamic characteristics of the flow at the nozzle exit plane (fig. 3).

F110-GE-129 Digital Engine Model

Flight and ground test data from the instrumented engine did not directly measure values of pressure, temperature, velocity, and mass flow at station 9. At station *jet*, these data did not provide the data needed for the evaluation of CTC and ANOPP codes. A digital engine performance model[†] was used to calculate some of the needed parameters. Others were computed using follow-on calculations.

Engine Model Description

The F110-GE-129 engine performance model (also referred to as the engine deck) is a digital computer FORTRAN program which predicts engine parameters and performance consistent with a nominal F110-GE-129 engine. The aerothermodynamic model calculates the various engine operating parameters. Many of these parameters would otherwise be difficult or impossible to measure because of the excessively high temperatures, inaccessibility of the area to instrumentation, or both.

Data Selection Procedure

Plots of selected flight parameters were compared with the times associated with the pilot call outs for the selected inbound distance, the overhead point, and the selected outbound distance. Results revealed that Mach number, altitude, *A8*, and PLA were the main parameters defining the quality of the data for a test run. A PLA and *A8,* which were constant along with a constant or slowly accelerating Mach number and a relatively constant altitude were needed. In the flight data tables, there are typically three data points per flyover: one at the start point, one at the overhead point, and one at the end point.

Engine Model Inputs

The F110-GE-129 engine deck input parameters used for the analysis consist of altitude, Mach number, *T1*, and PLA. The aircraft total temperature probe was inoperative for the acoustics flights, and it was planned to use the *T1*. For verification, the engine deck-calculated ambient temperature was compared with the temperature measured by the AFFTC weather balloon at approximately the time of flights 1 and 3. Figure 7 compares the ambient temperatures calculated from the flight *T1* measurement with the weather balloon-measured data as a function of altitude. Standard day *T1* is shown for reference. The flight and balloon comparisons match well enough to justify the use of *T1* in combination with aircraft-calculated Mach number and altitude.

[†]Wills, T. K., Cycle Deck User's Manual for F110-GE-129 Performance, GE R89AEB216, May 1989. (Contact General Electric Company, Lynn, Massachusetts.)

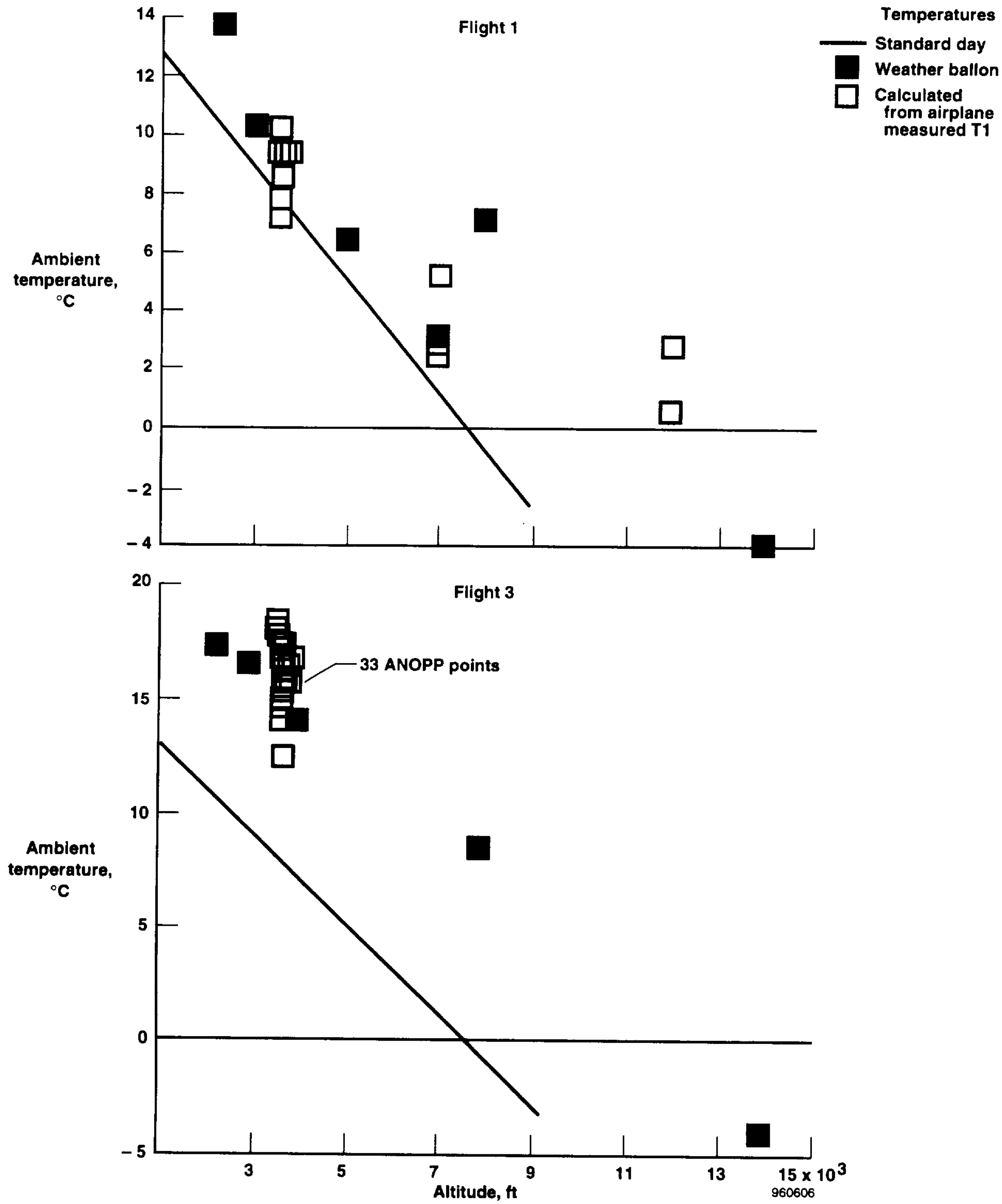

Figure 7. Ambient temperature and standard day temperature for the acoustics flyover tests.

The engine deck uses Mach number and ambient pressure based on altitude to compute the free stream total pressure. The inlet pressure recovery curve for the F-16XL, ship 2 (fig. 2(b)), was input into the engine deck to provide the correct engine face pressure recovery.

Engine Model Output

The engine deck, models the engine as a gas generator and predicts output flight parameters based on the measured airplane flight parameters which were previously input. Some of the unmeasureable parameters that were calculated by the engine deck and were needed for the acoustic analysis were gross thrust (*Fg*); *Vjet*; NPR; ratio of exhaust nozzle effective exit-plane area to its effective throat area, *AE9/AE8*; ratio of exhaust nozzle flow exit-plane static pressure to ambient static pressure, *Ps9/Pamb*; exhaust nozzle mixed-jet total temperature at the throat, *T8*; mass flow rate at the exhaust nozzle throat, *W8*; and other useful exhaust nozzle exit stream parameters, such as throat total pressure, *P8* and the specific heat ratio of exhaust gas at nozzle entrance, GAM7. The engine deck also calculates parameters, such as *PT2.5*, *Ps3*, *WFE*, *N1*, *N2*, and *A8* which may be compared to the engine measurements.

In addition to the engine deck-calculated value of *Vjet*, the local values of *V9*, *M9*, and *Mjet* were determined from later calculations.

Exhaust Flow Properties

For these calculations, steady, one-dimensional, adiabatic, isentropic flow was assumed to exist between the planes of the nozzle inlet (station 7) and the nozzle exit (station 9). One of three possible cases is assumed to exist at the nozzle exit plane depending on the level of static pressure (*Ps9*) existing at the moment of data sampling. If the condition ($Ps9 < Pamb$) exists, the flow is said to be overexpanded. If the condition ($Ps9 = Pamb$) exists, the flow is said to be fully expanded. When the condition ($Ps9 > Pamb$) exists, the flow is said to be underexpanded. In all cases, it is assumed that total temperature and specific heat ratio of exhaust gas is equal at stations 7, 8, 9, and *jet*.

Ideal or *Jet* Expansion Parameters

One way to calculate exhaust properties is to assume that the total pressure at the nozzle throat is isentropically expanded to atmospheric pressure. These *jet* parameters are independent of the nozzle expansion ratio and are only a function of NPR. The *Mjet* parameter uses this assumption.

Area Ratio Parameters

M9 is another parameter of interest for acoustic analysis. This parameter is determined based entirely on the ratio of the exhaust nozzle area at the exit plane to its area at the throat, *A9/A8*. It assumes that the flow expands isentropically from the throat to the exit regardless of what the exit static pressure may be. For the engine deck, an effective area ratio, *AE9/AE8* is calculated and may be used to calculate *M9*. This calculation is only useful for cases in which the flow at station 8 is choked.

Exhaust Static Temperature

The exhaust nozzle exit and fully expanded *jet* static temperatures, *Ts9* and *Tsjet*, are calculated from *T8* using GAM7 from the engine deck.

Local Speed of Sound and Exhaust Velocities

The speed of sound propagation in the hot gas stream was calculated using conventional gas dynamics relationships, then multiplied by the Mach number to arrive at the exhaust velocities. These calculations were performed in a follow-on program to supplement the engine deck outputs.

RESULTS AND DISCUSSION

The results of the ground run, CTC tests, and ANOPP tests are presented in tables 4, 5, and 6. Each table shows first, in part (a), the measured input data and measured engine parameters; second, in part (b), a comparison of the engine deck-calculated values to the engine measurements; and third, in part (c), the engine deck and follow-on calculated exhaust parameters. For the flyovers, there are usually three data points: one at the beginning of the run, one at the overhead point, and one at the end.

Table 4. F-16XL, ship 2, ground run test.
(a) Measured and engine deck-calculated parameters.

Mach number 0.0, pressure altitude = 2270 ft													
	Input to deck			Deck output		Measured engine parameters							
Test point	PLA, deg	*Tamb*, °R	*Pamb*, lbf/in^2	*T1*, °R	*P1*, lbf/in^2	*PT2.5*, lbf/in^2	*Ps3*, lbf/in^2	*WFE*, lb/h	*N1*, rpm	*N2*, rpm	EGT, °R	*A8*, in^2
1	20.4	517.6	13.53	517.6	13.2	15.9	53	1179	3141	10354	1456	965
2	24.7	517.6	13.53	517.6	13.1	17.5	71	1587	3992	11126	1426	770
3	30.5	517.6	13.53	517.6	13.0	21.0	108	2513	5113	11899	1445	520
4	32.5	517.6	13.53	517.6	12.9	21.8	116	2663	5341	12062	1530	519
5	38.7	517.6	13.53	517.6	12.8	24.6	145	3481	6051	12529	1542	496
6	43.9	517.6	13.53	517.6	12.6	26.5	168	4062	6491	12846	1580	491
7	48.9	517.6	13.53	517.6	12.5	28.1	185	4578	6858	13117	1631	489
8	55.1	517.6	13.53	517.6	12.3	30.1	207	5310	7207	13445	1678	492
9	60.2	517.6	13.53	517.6	12.1	31.7	227	6042	7510	13765	1732	499
10	67.6	517.6	13.53	517.6	12.0	33.8	251	6882	7693	14033	1793	482
11	72.8	517.6	13.53	517.6	11.8	36.7	287	8197	7860	14339	1899	444
12	83.6	517.6	13.53	517.6	11.4	38.5	312	9427	8187	14663	1999	445
13	85.2	517.6	13.53	517.6	11.4	38.3	314	9385	8215	14710	1996	444
14	53.7	517.6	13.53	517.6	12.4	29.7	205	5116	7135	13414	1628	488
15	29.7	517.6	13.53	517.6	13.0	20.4	104	2276	4972	11859	1379	546
16	15.2	517.6	13.53	517.6	13.2	15.9	52	1201	3111	10400	1497	975

Table 4. Continued.

(b) Comparison of measured and engine deck-calculated engine parameters.

Test point	PLA, deg	*PT2.5*, lbf/in^2		*Ps3*, lbf/in^2		*WFE*, lb/h		*N1*, rpm		*N2* rpm		*A8*, in^2	
		Meas	Deck	Meas	Deck	Meas	Deck	Meas	Deck	Meas	Deck	Meas	Deck
1	20.4	15.9	16.2	52.5	50.0	1179.1	1117	3141	3105	10354	10187	965	958
2	24.7	17.5	17.8	71.3	70.7	1587.3	1434	3992	3961	11126	11137	770	761
3	30.5	21.0	21.0	108.1	107.1	2512.9	2233	5113	5094	11899	11950	520	520
4	32.5	21.8	21.8	115.7	115.0	2663.4	2420	5341	5253	12062	12094	519	520
5	38.7	24.6	24.7	145.3	146.0	3480.9	3227	6051	6052	12529	12590	496	490
6	43.9	26.5	26.7	167.6	167.0	4061.8	3803	6491	6500	12846	12858	491	485
7	48.9	28.1	28.3	184.6	184.0	4578.1	4298	6858	6872	13117	13083	489	485
8	55.1	30.1	30.5	207.1	209.0	5309.9	5049	7207	7235	13445	13442	492	487
9	60.2	31.7	32.4	227.3	232.0	6041.9	5814	7510	7520	13765	13733	499	491
10	67.6	33.8	34.6	251.3	260.0	6881.9	6728	7693	7740	14033	14079	482	477
11	72.8	36.7	37.0	287.3	290.0	8196.8	7760	7860	7887	14339	14423	444	448
12	83.6	38.5	39.7	312.5	325.0	9427.0	9191	8187	8224	14663	14696	445	448
13	85.2	38.3	39.9	313.8	327.0	9384.8	9262	8215	8241	14710	14709	444	449

Table 4. Concluded.

(c) Deck output and calculated exhaust parameters.

								Exhaust properties					
								Station 9, f(*A9/A8*)				*Jet*, f(NPR)	
Test point	PLA, deg	*P8*, lbf/in^2	*T8*, °R	GAM7	*Fg*, lbf	*W8*, lb/sec	*AE9/AE8*	*M9*	*V9*, ft/sec	*Ps9/Pamb*	NPR	*Mjet*	*Vjet*, ft/sec
1	20.4	13.8	852	1.386	466	67.4	1.298	–	–	–	1.019	0.173	232
2	24.7	14.2	848	1.387	1028	89.1	1.261	–	–	–	1.053	0.279	385
3	30.5	16.7	918	1.382	2753	114.9	1.121	–	–	–	1.233	0.561	800
4	32.5	17.1	929	1.381	3079	121.2	1.121	–	–	–	1.263	0.594	849
5	38.7	19.4	991	1.377	4537	140.2	1.100	1.372	1804.1	0.47	1.436	0.746	1082
6	43.9	21.0	1032	1.374	5498	151.9	1.096	1.362	1831.0	0.52	1.550	0.826	1210
7	48.9	22.2	1065	1.372	6302	161.3	1.096	1.362	1859.3	0.55	1.642	0.882	1302
8	55.1	24.0	1115	1.368	7426	173.2	1.097	1.364	1904.7	0.59	1.770	0.952	1423
9	60.2	25.6	1165	1.364	8478	153.6	1.100	1.368	1950.9	0.63	1.890	1.011	1529
10	67.6	28.2	1233	1.359	9732	191.5	1.090	1.348	1984.8	0.72	2.088	1.095	1682
11	72.8	31.9	1321	1.353	11049	195.3	1.068	1.300	1998.4	0.87	2.360	1.194	1867
12	83.6	34.6	1411	1.347	12626	206.8	1.070	1.305	2070.6	0.94	2.559	1.258	2009
13	85.2	34.7	1415	1.346	12696	207.3	1.071	1.307	2076.4	0.94	2.567	1.261	2015
14	53.7	23.5	1101	1.369	7133	170.2	1.097	1.360	1888.8	0.58	1.737	0.935	1392
15	29.7	16.3	906	1.383	2503	111.7	1.132	–	–	–	1.203	0.527	748
16	15.2	13.8	852	1.386	457	67.5	1.300	–	–	–	1.018	0.170	227

Table 5. CTC test data.
(a) CTC measured and input to deck data.

		Measured and calculated inputs to deck				Calculated by deck			Measured engine data						
Test	Segment	PLA, deg	Mach number	Altitude, ft	T1, °R	*Tamb*, °R	*Pamb*, lbf/in^2	*P1*, lbf/in^2	PT2.5, lbf/in^2	*Ps3*, lbf/in^2	*WFE*, lb/h	*N1*, rpm	*N2*, rpm	EGT, °R	*A8*, in^2
A	Start	85.0	0.344	3565	520.9	508.9	12.90	13.72	45.6	381	10789	8305	14686	1846	446
A	OH	85.0	0.557	3610	538.5	507.1	12.88	15.58	53.2	440	12911	8470	14936	2153	446
A	End	85.0	0.758	3603	563.4	505.3	12.89	18.47	61.8	500	14654	8536	15060	2027	447
B	Start	85.1	0.622	7042	540.1	501.3	11.32	14.18	49.3	410	12071	8470	14887	1920	446
B	OH	85.0	0.852	7040	569.6	497.4	11.32	17.83	58.9	477	13869	8547	15044	2156	447
B	End	85.0	0.945	7035	585.5	496.8	11.33	19.73	63.1	501	14853	8566	15029	2190	447
C	OH	85.0	0.684	11975	543.4	496.9	09.36	12.54	42.6	356	10724	8486	14866	1998	445
C	End	85.0	0.946	12060	581.3	493.1	09.32	16.26	52.5	422	12442	8556	15044	2160	447
D	Start	85.1	0.329	3498	521.3	510.3	12.93	13.66	44.9	376	11033	8300	14607	1821	446
D	OH	85.1	0.563	3540	541.6	509.3	12.91	15.69	53.7	447	13005	8492	14960	2130	446
D	End	85.1	0.755	3558	563.6	486.1	12.90	18.45	61.4	499	12957	8520	15094	2136	446

Table 5. Continued.
(b) Comparison of measured and deck-calculated engine parameters.

Test	Segment	PLA, deg	Mach number	*PT2.5*, lbf/in^2		*Ps3*, lbf/in^2		*WFE*, lb/h		*N1*, rpm		*N2*, rpm		*A8*, in^2	
				Meas	Deck	Meas	Deck	Meas	Deck	Meas	Deck	Meas	Deck	Meas	Deck
A	Start	85.0	0.344	45.6	47.9	381	395	10789	11099	8305	8295	14686	14775	446	450
A	OH	85.0	0.557	53.2	55.0	440	456	12911	13161	8470	8469	14936	15034	446	451
A	End	85.0	0.758	61.8	63.0	500	511	14654	14797	8536	8535	15060	15098	447	452
B	Start	85.1	0.622	49.3	50.9	410	420	12071	12173	8470	8476	14887	15049	446	450
B	OH	85.0	0.852	58.9	59.9	477	482	13869	13834	8547	8542	15044	15039	447	452
B	End	85.0	0.945	63.1	64.2	501	508	14853	14609	8566	8561	15029	15078	447	452
C	OH	85.0	0.684	42.6	44.1	356	392	10724	10577	8486	8490	14866	15066	445	450
C	End	85.0	0.946	52.5	53.7	422	456	12442	12357	8556	8556	15044	15074	447	447
D	Start	85.1	0.329	44.9	47.6	376	392	11033	11020	8300	8287	14607	14772	446	449
D	OH	85.1	0.563	53.7	55.3	447	456	13005	13208	8492	8482	14960	15057	446	451
D	End	85.1	0.755	61.4	64.4	499	529	14700	15215	8520	8482	15094	15009	446	452

Table 5. Concluded.
(c) CTC deck and calculated parameters.

										Exhaust characteristics					
										Station 9, f(*AE9/AE8*)				*Jet*, f(NPR)	
Test	Segment	PLA, deg	Mach number	*P8*, lbf/in^2	*T8*, °R	GAM7	*W8*, lb/sec	*Fg*, lb	*AE9/AE8*	*M9*	*V9*, ft/sec	*Ps9/Pamb*	NPR	*Mjet*	*Vjet*, ft/sec
A	Start	85.0	0.344	41.8	1422	1.346	248.5	16793	1.199	1.520	2328	0.88	3.24	1.428	2223
A	OH	85.0	0.557	48.2	1480	1.342	280.5	20401	1.224	1.553	2412	0.96	3.74	1.528	2382
A	End	85.0	0.758	54.4	1488	1.342	319.3	24189	1.224	1.553	2419	1.09	4.22	1.610	2478
B	Start	85.1	0.622	44.5	1484	1.342	258.7	19145	1.223	1.553	2415	1.01	3.93	1.562	2422
B	OH	85.0	0.852	51.2	1481	1.343	304.2	23416	1.224	1.553	2413	1.17	4.52	1.656	2519
B	End	85.0	0.945	54.4	1484	1.342	325.2	25462	1.224	1.553	2416	1.24	4.80	1.696	2562
C	OH	85.0	0.684	38.5	1489	1.342	224.2	16852	1.223	1.552	2418	1.06	4.11	1.593	2460
C	End	85.0	0.946	46.0	1496	1.342	269.9	21343	1.221	1.549	2421	1.28	4.93	1.713	2590
D	Start	85.1	0.329	41.6	1421	1.346	247.1	16647	1.194	1.510	2317	0.88	3.22	1.423	2216
D	OH	85.1	0.563	48.3	1493	1.342	281.2	20488	1.224	1.553	2423	0.97	3.74	1.529	2386
D	End	85.1	0.755	55.7	1466	1.343	330.8	25016	1.224	1.553	2401	1.11	4.32	1.625	2474

Table 6. ANOPP flyover test data.
(a) ANOPP flyover measured input data to deck.

		Engine data													
		Measured and calculated inputs to deck				Calculated by deck			Measured engine parameters						
Test	Segment	PLA deg	Mach number	Altitude, ft	*T1*, °R	*Tamb*, °R	*Pamb*, lbf/in^2	*P1*, lbf/in^2	*PT2.5*, lbf/in^2	*Ps3*, lbf/in^2	*WFE*, lb/h	*N1*, rpm	*N2*, rpm	EGT, °R	*A8*, in^2
E	Start	48.5	0.308	3783	530.0	520.1	12.79	13.40	30.3	201.1	4736	6948	13314	1620	478
E	OH	48.5	0.300	3730	530.3	520.9	12.82	13.37	30.1	200.0	5285	6936	13304	1608	480
E	End	48.5	0.282	3648	529.1	520.8	12.86	13.31	29.9	198.5	4619	6937	13290	1607	478
F	Start	35.1	0.603	3780	558.6	520.7	12.80	16.03	31.8	194.2	4360	6396	13321	1576	463
F	OH	35.1	0.601	3740	559.0	521.3	12.82	16.03	31.8	193.8	4332	6388	13316	1579	463
F	End	34.8	0.605	3750	561.3	523.0	12.81	16.08	31.8	194.0	4332	6381	13318	1565	459
G	Start	46.6	0.793	3728	584.5	519.2	12.82	19.02	43.5	289.3	7148	7317	14069	1741	469
G	OH	46.6	0.804	3735	586.5	519.4	12.82	19.23	43.8	291.1	7221	7306	14064	1741	469
G	End	46.6	0.814	3770	589.1	520.2	12.80	19.39	43.8	293.2	7185	7308	14079	1757	468
H	Start	55.5	0.946	3753	610.9	518.2	12.81	22.34	54.8	379.8	9992	7815	14576	1882	471
H	OH	55.6	0.955	3745	611.8	517.5	12.81	22.57	55.3	382.0	9864	7823	14590	1747	474
H	End	55.5	0.947	3742	611.8	518.8	12.82	22.37	54.8	379.5	9864	7806	14576	1719	472

Table 6. Continued.
(b) Comparison of measured and deck-calculated parameters.

Test	Segment	PLA, deg	Mach number	*PT2.5*, lbf/in^2		*Ps3*, lbf/in^2		*WFE*, lb/h		*N1*, rpm		*N2*, rpm		*A8*, in^2	
				Meas	Deck	Meas	Deck	Meas	Deck	Meas	Deck	Meas	Deck	Meas	Deck
E	Start	48.5	0.308	30.3	30.0	201.1	195.4	4736	4506	6948	6927	13314	13219	478	476
E	OH	48.5	0.300	30.1	30.0	200.0	195.0	5285	4497	6936	6926	13304	13221	480	476
E	End	48.5	0.282	29.9	29.9	198.5	194.1	4619	4472	6937	6918	13290	13206	478	476
F	Start	35.1	0.603	31.8	31.9	194.2	190.0	4360	4229	6396	6344	13321	13101	463	458
F	OH	35.1	0.601	31.8	31.9	193.8	190.0	4332	4227	6388	6345	13316	13104	463	458
F	End	34.8	0.605	31.8	31.7	194.0	188.0	4332	4182	6381	6319	13318	13103	459	458
G	Start	46.6	0.793	43.5	43.8	289.3	288.0	7148	6922	7317	7288	14069	13895	469	458
G	OH	46.6	0.804	43.8	44.2	291.1	290.0	7221	6981	7306	7290	14064	13911	469	457
G	End	46.6	0.814	43.8	44.5	293.2	291.0	7185	7022	7308	7292	14079	13932	468	456
H	Start	55.5	0.946	54.8	55.3	379.8	381.0	9992	9722	7815	7803	14576	14490	471	467
H	OH	55.6	0.955	55.3	55.9	382.0	385.0	9864	9834	7823	7809	14590	14497	474	468
H	End	55.5	0.947	54.8	55.3	379.5	381.0	9864	9719	7806	7804	14576	14492	472	467

Table 6. Concluded.
(c) ANOPP test engine deck and calculated outputs.

										Exhaust conditions					
										Station 9, f(*AE9*/*AE8*)				*Jet*, f(NPR)	
Test	Segment	PLA, deg	Mach number	*P8*, lbf/in^2	*T8*, °R	GAM7	*Fg*, lb	*W8*, lb/sec	*AE9*/*AE8*	*M9*	*V9*, ft/sec	*Ps9*/*Pamb*	NPR	*Mjet*	*Vjet*, ft/sec
E	Start	48.5	0.308	23.58	1078	1.371	7400	170	1.089	1.35	1859	0.63	1.843	0.985	1444
E	OH	48.5	0.300	23.53	1078	1.371	7363	169	1.090	1.35	1859	0.63	1.836	0.981	1440
E	End	48.5	0.282	23.43	1076	1.371	7288	169	1.090	1.35	1857	0.62	1.822	0.975	1430
F	Start	35.1	0.603	25.14	1057	1.373	7934	175	1.076	1.32	1810	0.70	1.965	1.039	1496
F	OH	35.1	0.601	25.13	1058	1.373	7918	175	1.076	1.32	1810	0.70	1.961	1.038	1494
F	End	34.8	0.605	25.00	1058	1.373	7840	174	1.076	1.32	1811	0.69	1.952	1.034	1490
G	Start	46.6	0.793	34.93	1188	1.363	13499	235	1.104	1.37	1973	0.91	2.724	1.298	1893
G	OH	46.6	0.804	35.24	1191	1.363	13665	236	1.108	1.38	1986	0.90	2.749	1.305	1902
G	End	46.6	0.814	35.46	1194	1.364	13787	237	1.112	1.39	1999	0.90	2.770	1.310	1911
H	Start	55.5	0.946	44.10	1290	1.356	19093	290	1.237	1.53	2227	0.91	3.443	1.468	2160
H	OH	55.6	0.955	44.57	1292	1.356	19373	293	1.237	1.53	2229	0.92	3.478	1.475	2169
H	End	55.5	0.947	44.11	1291	1.356	19091	290	1.237	1.53	2228	0.91	3.442	1.468	2160

Verification of F110-GE-129 Engine Deck

Use of the F110-GE-129 engine deck, which represents a nominal engine, could introduce errors if the flight test engine were significantly different from the assumed nominal engine. To assess such potential errors, a comparison of some engine-measured parameters with calculated parameters from the engine deck was made. Tables 4(b), 5(b), and 6(b) compare the airplane-measured parameters with the engine deck-calculated parameters. There are six measured engine parameters (in addition to the PLA, *T1*, altitude, and Mach number that are inputs to the engine deck) that may be compared with engine deck-calculated parameters. These are *N1*, *N2*, *PT2.5*, *Ps3*, *WFE*, and *A8*. Inspection of these tables shows very good agreement for these comparisons, indicating that the engine deck is a good representation of the engine flown in the F-16XL, ship 2. Plots of the comparisons are shown in figure 8 for the ground run, figure 9 for the CTC tests, and fig 10 for the ANOPP tests. The ground run, CTC, and ANOPP flyover data show good to excellent agreement between measured and calculated engine parameters.

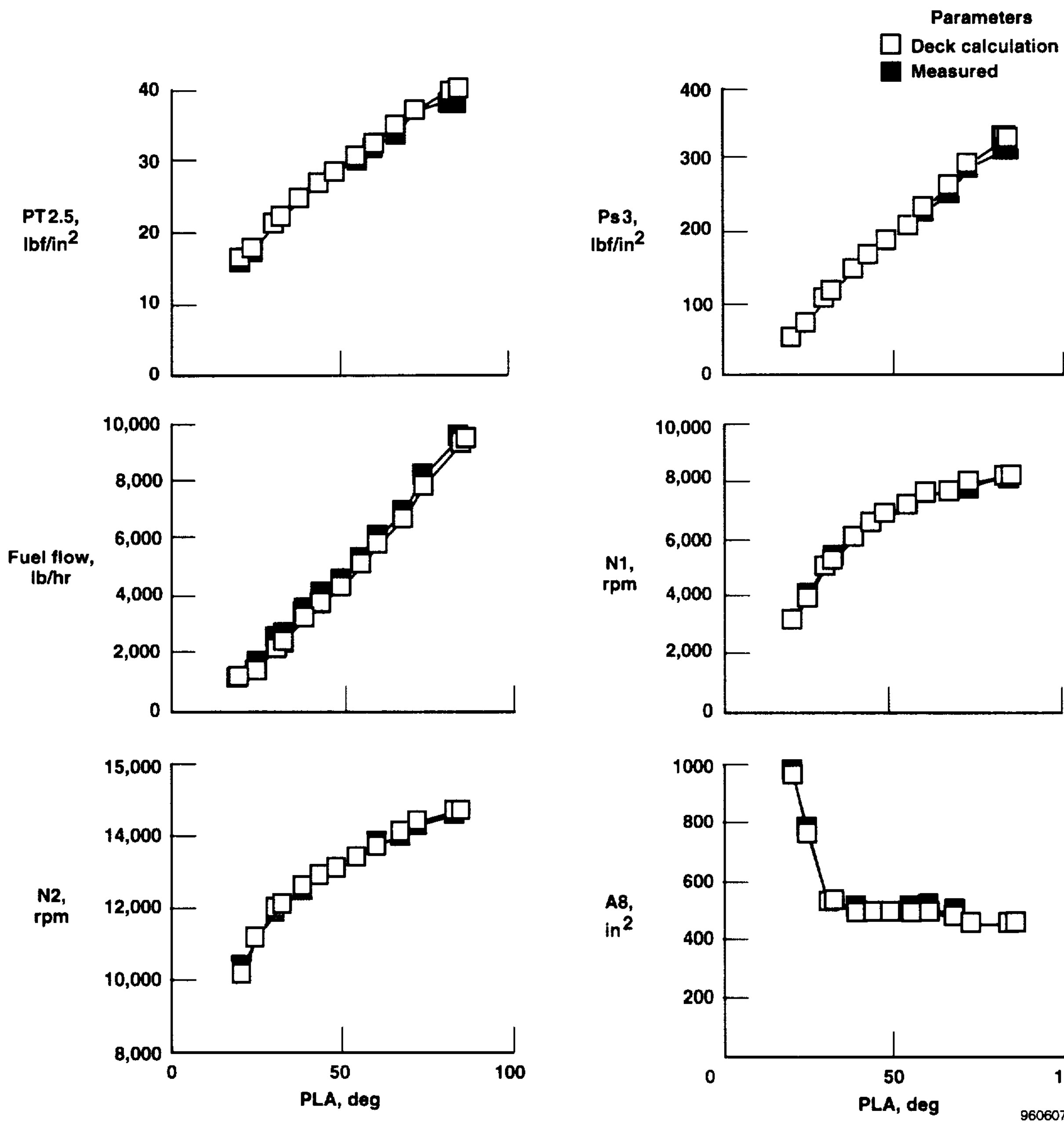

Figure 8. Comparison of measured and deck-calculated parameters, ground run.

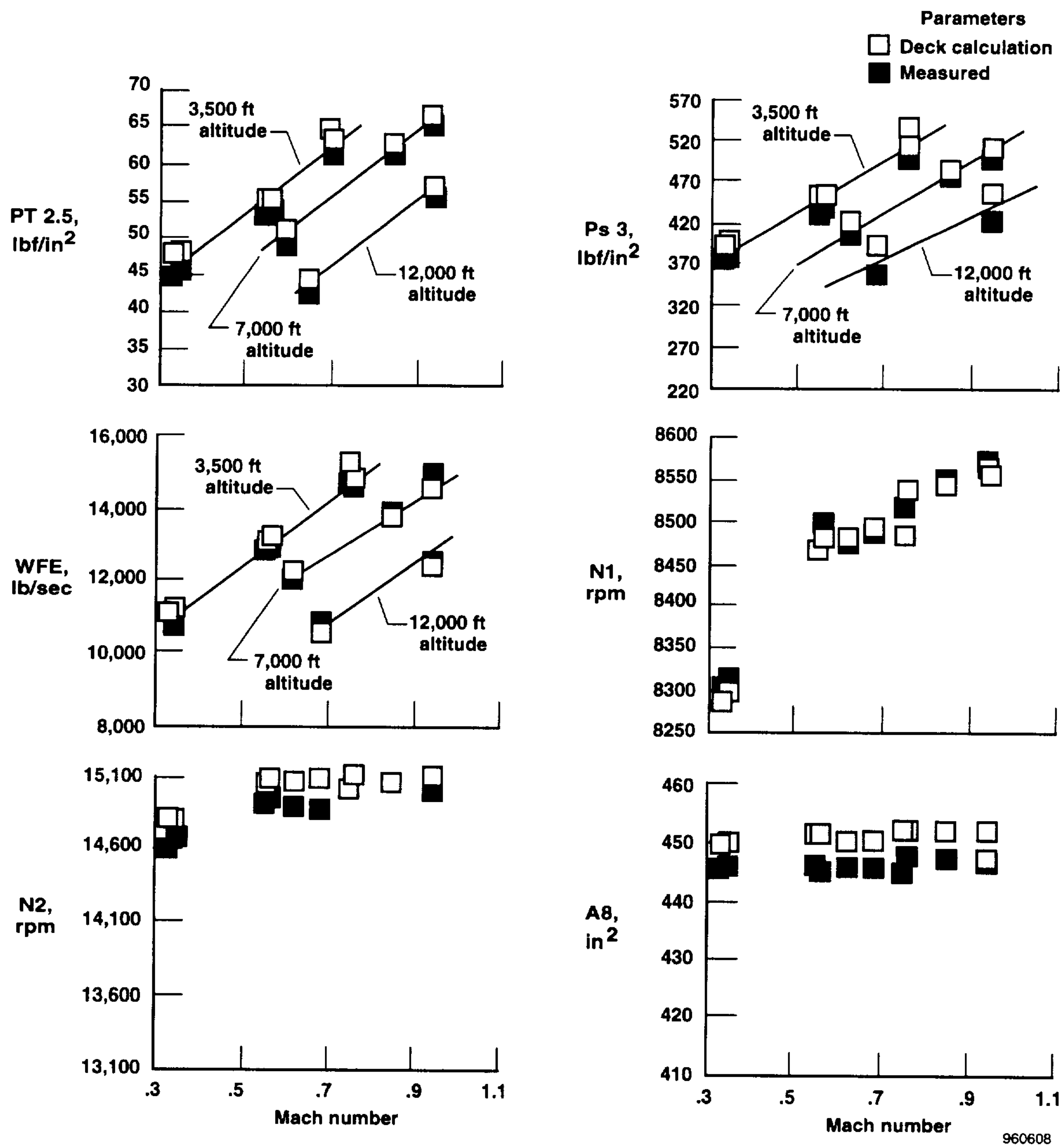

Figure 9. Comparison of measured and deck-calculated parameters, climb-to-cruise tests.

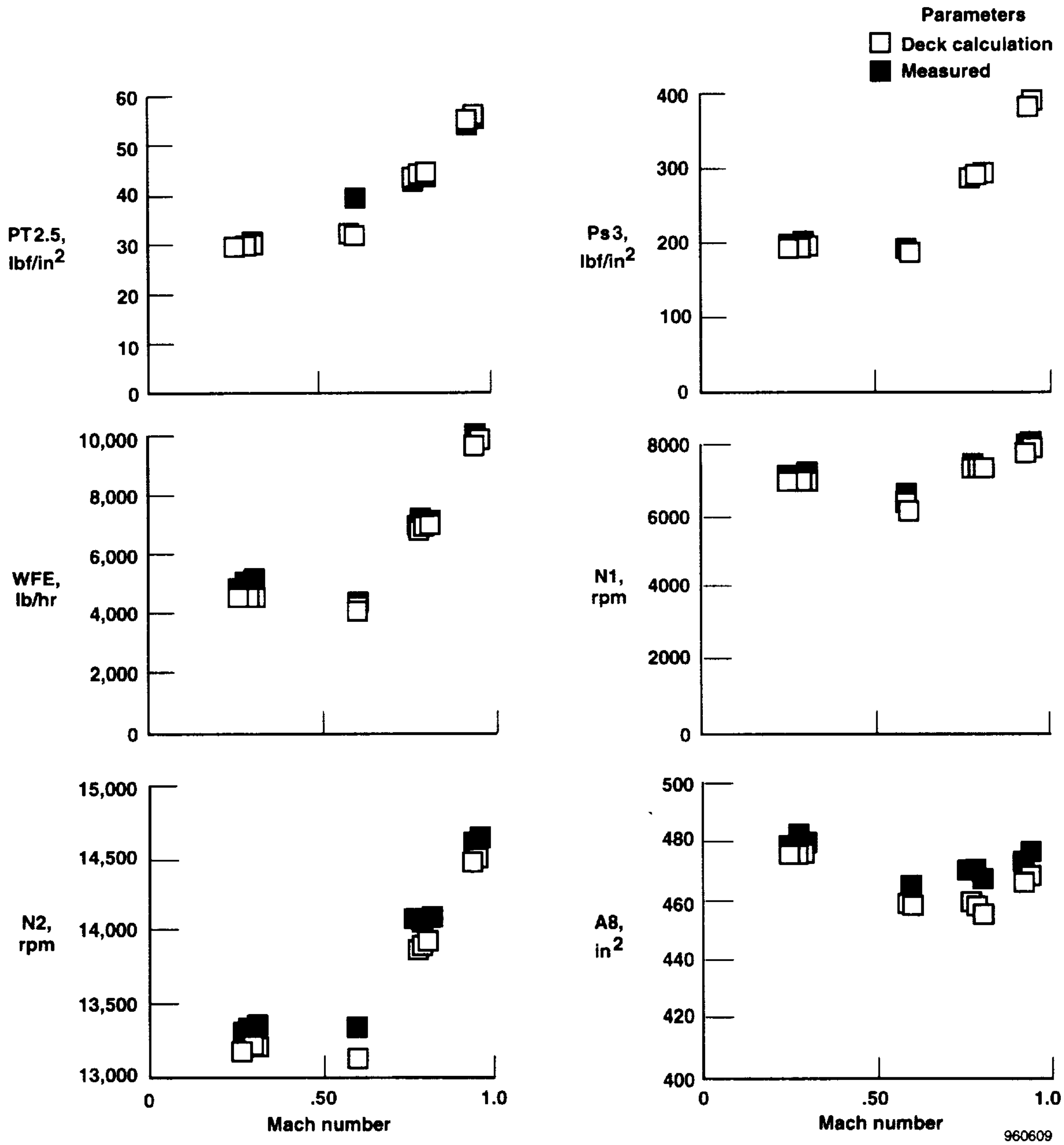

Figure 10. Comparison of measured and deck-calculated parameters, ANOPP tests.

Another indication of the quality of these engine deck data may be inferred from figure 7 which shows temperatures of no more than 10 °C from standard day temperature and not much variation for the 2 test days. Cycle decks tend to be less accurate as deviations from standard day temperature (where much of the cycle deck data were obtained) increase.

Ground Static Test Results

The ground static run data are listed in table 4 for the range of power settings from idle to intermediate. Note that the nozzle is unchoked below a PLA of 38° and is overexpanded for all ground conditions. Maximum NPR is 2.57 at intermediate power.

Figure 11 plots these values for *Mjet* and *M9* versus PLA for the test points where the flow is choked. The *M9* and *Mjet* are separated at the lower values of PLA and approach each other at the higher PLA where the nozzle is only slightly overexpanded. The corresponding values of *V9* and *Vjet* are also plotted showing similar trends to the Mach numbers.

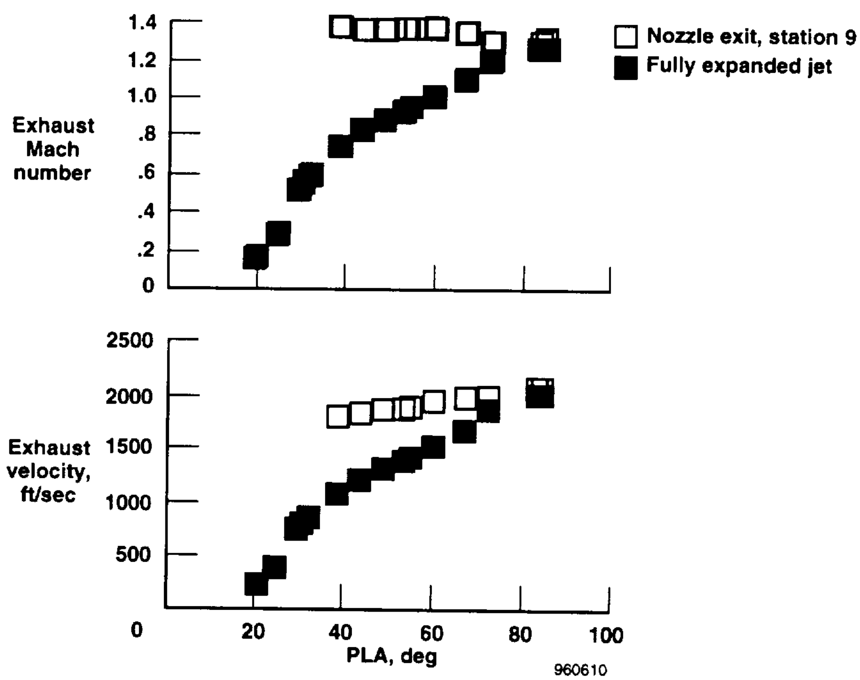

Figure 11. Exhaust flow properties, F110-GE-129 engine in F-16XL, ship 2, ground run.

Flyover Exhaust Flow Properties Results

For most flyover tests, three data points per run are shown: the initial data at the beginning of the run, a point over the microphone array, and the last point at the end of the data run. Table 3 shows a summary of the flyover tests from the three flights. The airplane accelerated rapidly for the CTC tests, while the ANOPP tests were at nearly constant Mach number.

CTC Test Results

Table 5 shows the measured and calculated parameters for the CTC tests. In all cases, the airplane accelerated significantly during the run. Values of NPR varied from 3.2 to almost 5.

Figure 12 shows *M9*, and *Mjet* for the CTC conditions and compares both the exhaust Mach numbers and velocities versus the aircraft free stream Mach number. Conditions shown in figure 12 are at intermediate power (PLA = 85°) and at nominal altitudes ranging from 3,800 to 12,300 ft. Because the nozzle area is essentially constant at intermediate power, *A9/A8* does not vary significantly; therefore, *M9* is almost constant at a value of 1.55. At the lower aircraft Mach numbers (below Mach 0.6), the nozzle flow is overexpanded as it was in the ground run, so *Mjet* < *M9*. Above Mach 0.6, the nozzle is underexpanded, and *Mjet* > *M9*. The effects of altitude were quite small as would be expected for *V9* and *Vjet*. Figure 12 shows a similar trend.

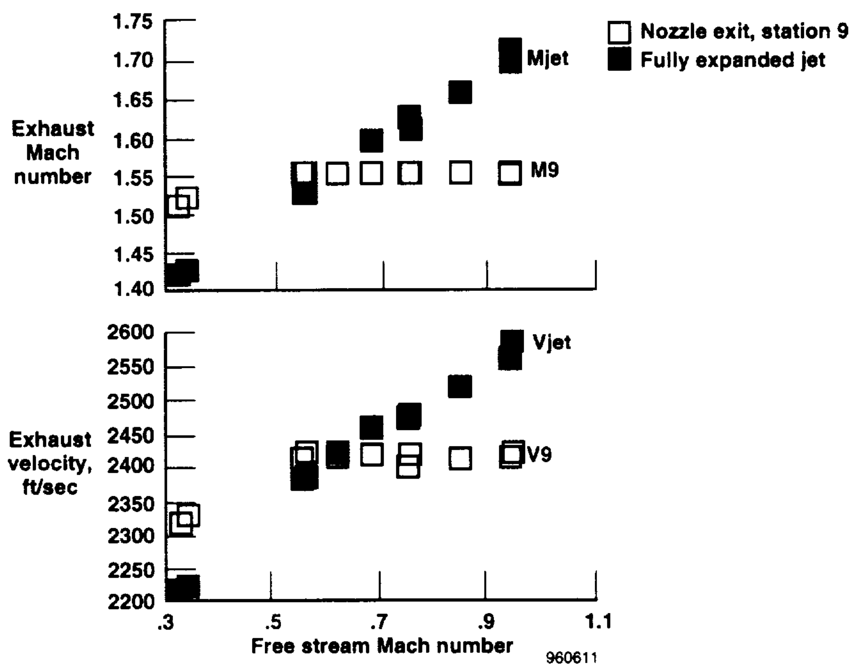

Figure 12. Exhaust flow properties, F110-GE-129 engine in F-16XL, ship 2, climb-to-cruise tests, all tests at intermediate power, for altitudes, see table 5.

ANOPP Test Results

Table 6 lists ANOPP test data from flight 3. The flight points were near an altitude of 3800 ft (1500 ft AGL) and were started two miles before and ended two miles past the microphone array. The PLA was fixed at PLF. Because of the lower power settings, ANOPP test NPR values varied from 1.8 to 3.4. A significant variation also existed in PLA, so the *A9/A8* parameter varied; hence, *M9* varied from 1.32 to 1.53.

Figure 13 shows the exhaust Mach number and velocity as a function of airplane Mach number. The *M9* is higher than *Mjet* (fig. 13(a)) because the flow is overexpanded at all conditions. Similarly, *V9* is higher than *Vjet*. At the higher Mach number conditions, the nozzle flow is only slightly overexpanded.

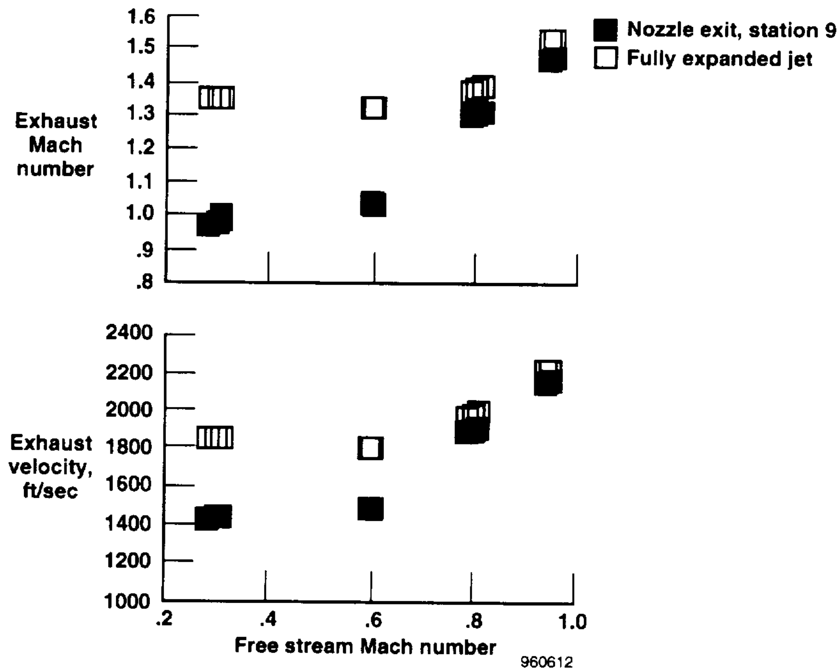

Figure 13. Exhaust flow properties, F110-GE-129 engine in F-16XL, ship 2, ANOPP tests, 3800 ft altitude.

CONCLUDING REMARKS

Flyover and static tests of the F-16XL, ship 2, airplane, powered by the GE F110-GE-129 engine, were conducted as part of a joint NASA Dryden and NASA Langley program to study the acoustics of high nozzle pressure ratio engines. An engine cycle deck was used to calculate parameters for comparison with measured parameters. The engine deck and follow-on calculations were also used to calculate exhaust properties where measurements were not possible. Very good agreement was found between cycle deck-calculated and measured engine parameters. Such agreement gives good confidence in the calculated exhaust properties. Nozzle pressure ratios up to almost 5 occurred at intermediate power, with a maximum jet Mach number of 1.7 and maximum jet velocity of nearly 2600 ft/sec. Nozzle conditions ranged from underexpanded to overexpanded, depending on flight conditions.

Dryden Flight Research Center
National Aeronautics and Space Administration
Edwards, California, August 1996

REFERENCES

1. Zorumski, William E., *Aircraft Noise Prediction Program Theoretical Manual*, NASA TM-83199, Part 1, 1982.

2 Ennix, Kimberly A., Burcham, Frank W., and Webb, Lannie D., *Flight-Determined Engine Exhaust Characteristics of an F404 Engine in an F-18 Airplane*, NASA TM-4538, 1993.

3 Ennix, Kimberly A., *Engine Exhaust Characteristics Evaluation in Support of Aircraft Acoustic Testing*, NASA TM-104263, 1993.

REPORT DOCUMENTATION PAGE

Form Approved
OMB No. 0704-0188

1. AGENCY USE ONLY (Leave blank)

2. REPORT DATE
November 1996

3. REPORT TYPE AND DATES COVERED
Technical Memorandum

4. TITLE AND SUBTITLE
Flight and Static Exhaust Flow Properties of an F110-GE-129 Engine in an F-16XL Airplane During Acoustic Tests

5. FUNDING NUMBERS
WU 505-68-10

6. AUTHOR(S)
Jon K. Holzman, Lannie D. Webb, and Frank W. Burcham, Jr.

7. PERFORMING ORGANIZATION NAME(S) AND ADDRESS(ES)
NASA Dryden Flight Research Center
P.O. Box 273
Edwards, California 93523-0273

8. PERFORMING ORGANIZATION REPORT NUMBER
H-2122

9. SPONSORING/MONITORING AGENCY NAME(S) AND ADDRESS(ES)
National Aeronautics and Space Administration
Washington, DC 20546-0001

10. SPONSORING/MONITORING AGENCY REPORT NUMBER
NASA TM-104326

11. SUPPLEMENTARY NOTES

12a. DISTRIBUTION/AVAILABILITY STATEMENT
Unclassified—Unlimited
Subject Category 07

12b. DISTRIBUTION CODE

13. ABSTRACT (Maximum 200 words)

The exhaust flow properties (mass flow, pressure, temperature, velocity, and Mach number) of the F110-GE-129 engine in an F-16XL airplane were determined from a series of flight tests flown at NASA Dryden Flight Research Center, Edwards, California. These tests were performed in conjunction with NASA Langley Research Center, Hampton, Virginia (LaRC) as part of a study to investigate the acoustic characteristics of jet engines operating at high nozzle pressure conditions. The range of interest for both objectives was from Mach 0.3 to Mach 0.9. NASA Dryden flew the airplane and acquired and analyzed the engine data to determine the exhaust characteristics. NASA Langley collected the flyover acoustic measurements and correlated these results with their current predictive codes. This paper describes the airplane, tests, and methods used to determine the exhaust flow properties and presents the exhaust flow properties. No acoustics results are presented.

14. SUBJECT TERMS
Acoustics; F110 engine; F-16XL airplane; Flyover noise

15. NUMBER OF PAGES
32

16. PRICE CODE
A03

17. SECURITY CLASSIFICATION OF REPORT	18. SECURITY CLASSIFICATION OF THIS PAGE	19. SECURITY CLASSIFICATION OF ABSTRACT	20. LIMITATION OF ABSTRACT
Unclassified	Unclassified	Unclassified	Unlimited

NSN 7540-01-280-5500

Available from the NASA Center for AeroSpace Information, 800 Elkridge Landing Road, Linthicum Heights, MD 21090; (301)621-0390

Standard Form 298 (Rev. 2-89)
Prescribed by ANSI Std. Z39-18
298-102